ISSN: 0976-9102 (ONLINE)
DOI: 10.21917/ijivp.2026.0551

SUPERVISED DEEP LEARNING ON HYBRID APPROACH OF COMPRESSED CONTOUR-INFORMED TEXTURE FEATURE APPROACH FOR PALMPRINT RECOGNITION

B. Abirami and K. Krishnaveni
Department of Computer Science, Sri S. Ramasamy Naidu Memorial College, India

Abstract

Biometric technology protects valuable assets and digital data by utilizing human physical and behavioral traits. Among these traits, palmprint recognition is recognized as particularly effective due to its unique characteristics. This paper introduces a new method called the Hybrid Approach of Compressed Contour Texture Analysis for Palmprint Recognition System with Supervised Deep Learning Classifier (HCCTA-SDLCNet) to enhance security in biometric systems. This method integrates the Hybrid approach of Compressed Contour Texture Analysis (HCCTA) for attribute extraction with the Supervised Deep Learning Classifier (SDLCNet). The process begins with the data normalization of a Two Dimensional Palmprint Region of Interest (2DPROI), followed by the capture of the Contour Pre-Processed Image of 2D-PROI Sample (CPI) using the Progressing Amalgamation of Conventional Compression (PACC) and the Canny edge detection model. The PACC combines the Discrete Wavelet Transform (DWT) and Principal Component Analysis (PCA) for sample compression, final in a Compressed Contour Preprocessed 2DPROI Image (CCPI). The HCCTA method focuses on extracting essential texture features from the CCPI. These extracted features are then analyzed using the SDLCNet classification model to identify individuals. The research utilizes 2DPROI data from the POLYU database at Hong Kong Polytechnic University. The intended system demonstrates a high benchmark, achieving 99.5% recognition accuracy, which is superior to existing biometric approaches.

Keywords:

Biometric Technology, Hybrid Approach of Compressed Contour Texture Analysis, Palmprint Recognition System, Two Dimensional Palmprint Region of Interest (2DPROI), Canny Edge Detection, Supervised Deep Learning Classifier, DWT, Principle Component Analysis

1. INTRODUCTION

Various Personal Identity Verification methods are necessary for ensuring security at national borders, controlling access, and maintaining safety in banks, airports, and other locations [1]. [2]This can be achieved through asset-based, knowledge-based, and biometric technologies for authentication and identification. However, asset-based and skill-based technologies are relatively easy to replicate and forget [1]. In contrast, biometric technology offers a more reliable and secure means of providing high-level protection for the public [1] [3].

Biometric systems offer a secure approach to confirming identity [4]. Biometric Authentication and Identification Systems (BAIS) are essential for safeguarding the growing digital environment of the IoT. The main scope of this study is to prepare accurate solutions for three main areas: first, to meet user demands for securing their electronic information and valuable assets cost-effectively and conveniently; second, to enhance security against unauthorized hacking attempts; and third, to develop a resilient system that prevents unauthorized entry into digital resources, BAIS operates as a live platform for identifying individuals in real time, achieved by collecting, analyzing, and evaluating digital data related to physical and logical human traits [5]. Researchers are investigating various biometric characteristics to develop effective BAIS.

Various biometric authentication systems have employed numerous traits, such as fingerprints, facial recognition, iris scans, signatures, and finger veins. Currently, palmprint recognition technology is advancing quickly [6]. This technology offers a reliable, user-friendly, and cost-effective method for automatic Personal Identity Verification [7][8]. Palmprints contain extensive information. Identification through palmprints involves sample processing and recognition techniques that analyze the palm's features. Unique textures and line traits of the palm remain constant over time, leading to increased interest among researchers.

Among the biometric traits, palmprint recognition stands out as a significant advancement in the field. Palmprint Visual data provide rich, distinctive features for identifying individuals, making it a crucial topic in biometric studies [9]. Palmprints consist of the skin patterns on the hand's underside, extending from the wrist to the fingers. Three major lines are present in the palm: the cognitive line, emotional line, and vitality line, formed by the natural flexing of the hand. These lines are key identifiers in palmprint analysis. Identifying palmprint features is essential for accurate recognition [10].

The principal lines and wrinkles of a human palm can be seen as edges or contours that provide attribute information. These edges differ from one palm to another. The Canny edge detection model effectively identifies a set of edges of varying sizes across an entire visual data[11].

[12] Data compression plays a crucial role in research related to sample and video processing. As computer and internet technology progresses, more multimedia content is shared online and through wireless networks. Transmitting raw data takes up significant bandwidth and requires extensive storage, making it necessary to encode this information using fewer bits through compression methods. It is equally important that these techniques can reconstruct the data closely to its original form. Effective compression and decompression models can achieve this. The DWT and Principal Component Analysis (PCA) are widely employed models. DWT allows for multi-resolution analysis and flexible compression, while Discrete Cosine Transform (DCT) may introduce false contour effects and blocking artifacts at higher compression rates [13]. [14] introduced a DWT and IDWT based improved image compression scheme with higher compression ratio and revealed wavelet transform approaches is suitable to compress the image size. [15] In this study, we also developed a hybrid compression

model combining the advantages of DWT, CHC and PCA. With the increasing use of image data, better image compression techniques achieved up to 60% compression while maintaining high visual quality. DWT, on the other hand, demands substantial computational resources. It is adept at providing sample sampling information at various locations and frequencies. High compression rates are achievable with DWT, which can separate the finer details of a sample through its wavelet functions [17]. [18] this study developed a hybrid compression model combining the advantages of DWT, CHC and PCA with the achievement of up to 60% compression while maintaining high visual quality. [16] The text discusses a method for image compression using discrete wavelet transform with Haar wavelet. It highlights the application of global principal component analysis on the LH and HL frequency sub-band images. This approach focuses on preserving essential boundaries and contours during the compression process, ensuring that minimal information is lost, particularly during the thresholding phase. The technique aims to enhance the efficiency of image compression while maintaining critical visual details. [19] Combining two or more compression techniques offers greater advantages than using just one, referred to as "Hybrid Approaches." [20]. [21] The paper presents the Compressed Contour Cumulative GLCM Texture Analysis Model based CNN for Palmprint Recognition (3CGLCM-CNNNet), achieving a 99% higher Accurate Authentication Rate (AAR) compared to existing methods in the field of biometric technology.

In the recognition phase, the system captures features of the palmprint and converts them into a digital format. This format is then processed by a attribute extractor to match the template representation. The final output is sent to a attribute matcher, which compares it with the templates to confirm the individual's identity.

Texture-based techniques, like DCT, are employed to extract features from palmprint Visual data [22]. Palmprints possess various texture features, making this technique a comprehensive method. Researchers focus on texture attribute extraction due to its effectiveness in deriving relevant content from individuals [23]. This paper [24] applies texture-based extraction methods for palmprint authentication, treating palm principle lines as texture components.

An optimized method for extracting texture features is the model-based texture approach because it requires less computation time and fewer processing steps compared to other methods [25] [26]. Model-based techniques highlight essential qualitative properties of textures [27] [28]. In 1970, Mandelbrot introduced fractals to model texture characteristics such as roughness and self-similarity [28]. Humeau-Heurtier intended a segmentation-based fractal analysis, which allows for efficient application of fractal models with lower computation time [29].

The FD method is commonly used for investigating textural patterns in various fields, including signature and palmprint recognition [30], [31]. Shi et al. [32] noted that fractal-based attribute extraction is effective in computer-aided diagnosis systems with large datasets. Gangepain and Roques-Carmes [33], [34] developed the Box-Counting model to estimate fractal dimensions. However, this method often yields the same dimension values for different textures. The lacunarity approach addresses this issue. [35] [36] [37] To distinguish texture patterns that exhibit the same fractal dimensions, Mandelbrot employed the Gliding-box model to define lacunarity based on variations in their statistical properties such as mean or variance

[38] analysed and exposed some reviews among the several feature extraction techniques, and it revealed statistical –based is more sensitive to noise and image distortion with low – computational complexity, filter-based texture extraction techniques provide more accuracy and precision in result. Statistical features are derived from the GLCM [39]. [40], [41], [42], [43] Texture-based attribute extraction methods typically include GLCM, Gabor filters, Haar filters, and Daubechies filters. [44] This study employed a hybrid feature extraction approach, which integrates both Gray-level co-occurrence matrix (GLCM) with Haralick and autoencoder features with an autoencoder and produced an accuracy of 99.89% in diagnostic and prognostic lung cancer treatment planning and decision-making systems. [45], [46]. The authors in another study applied the GLCM method to capture textural information related to gray-level spatial dependencies in Visual data. [47] From the GLCM obtained, several texture-based statistical parameters can be calculated using different formulas, achieving a classification accuracy of 97% with Convolutional CNN. We put forth a hybrid method that combines both review-level and aspect-level features to form a new hybrid feature vector for each sentiment review. Sentiment was classified through an LSTM model with an average precision of 94.46% in consumer sentiment analysis.A cluster of encoded attributes is extracted and recorded in order to support identification and recognition procedure based on Machine Learning (ML) and Deep Learning (DL) classifiers belonging to the Artificial Intelligence (AI) domain [48]. Earlier findings indicated that the feed-forward neural network, when trained with back-propagation, reached an identification accuracy of 99.99%, exceeding the results of other machine learning models explored [49]. Meanwhile, another study had shown that deep learning-based models achieved higher recognition accuracies on palmprint images (visual) [43]. [50] This paper scrutinized and discussed the advantages, limitations, and research opportunities of ML support in manufacturing using 114 journal articles containing the terms of supervision approaches, function, ML algorithm, data inputs and outputs, and application domain.

Although machine learning models are very accurate in the prediction of outcomes based on available information, the difficulty of machine learning models in handling large amounts of data make the decision process less transparent and understandable. To address these shortcomings, one has witnessed more focus on deep learning classifiers [51]. Deep Learning on large datasets demonstrated impressive performance in other domains like healthcare and biometrics, aided by including advanced techniques that could enhance both the training efficiency and accuracy [52].

This paper introduces a novel proficient PRS model called HCCTA-SDLC$_{Net}$. It presents innovative methods for extracting sample attribute values and classifying them, referred to as the HCCTA attribute extraction method and the SDLC$_{Net}$ classifier method. These methods are outlined in section 2. Both approaches enable efficient computation by calculating lacunarity values and Haralick's attribute values through the Gliding Box model and the GLCM technique. Section 3 and section 4 provide detailed

experimental analysis and performance evaluation of the HCCTA-SDLC$_{Net}$ PRS model.

2. INTENDED METHODOLOGY

The HCCTA-SDLC$_{Net}$ model operates through four levels: 1. Data acquiring level, 2. Data normalization, 3. Attribute extraction, and 4. Image labeling or correlation. The recognition and verification workflows of the HCCTA-SDLC$_{Net}$ model are in Fig.1 and Fig.2.

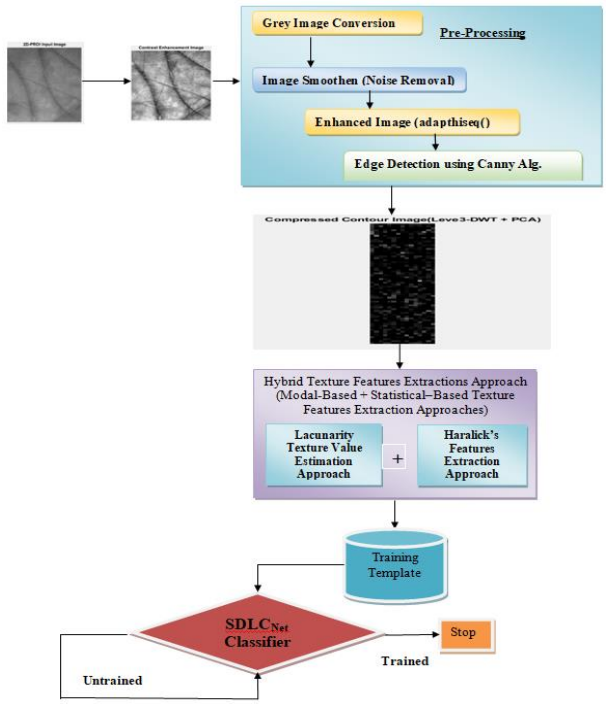

Fig.1. Architectural Diagram of HCCTA-SDLCNet Model Recognition Process

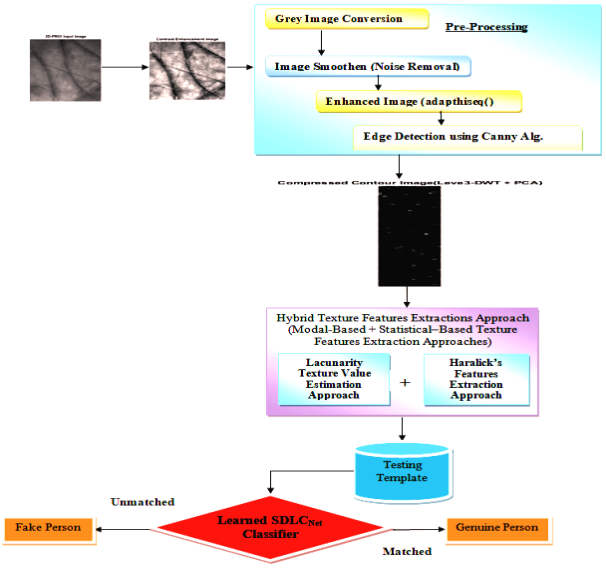

Fig.2. Architectural Diagram of HCCTA-SDLCNet Model Verification Process

2.1 DATA ACQUIRING LEVEL

This research employs data from the PolyU Multi-spectral 2DPROI palmprint database, which consists of 8000 normalized 2DPROI palmprint visual data in .bmp format. These visual data are derived from the palms of 400 volunteers, with 400 sets in total, split equally between two hands. The visual data are grouped into two distinct sections, each containing 10 visual data of either right- or left-hand palm. The Fig.3 depicts the few sample 2DPROI images.

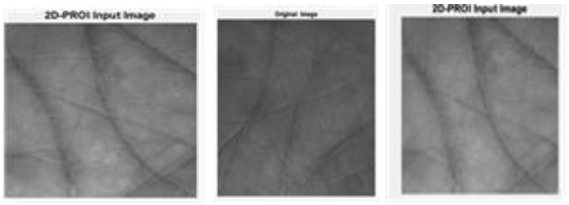

Fig.3. Sample Input 2DPROI Visual Data of PolyU Dataset

2.2 DATA NORMALIZATION LEVEL

Data normalization is essential to enhance the quality of the input sample for further analysis. During this stage, unnecessary data is removed to accurately assess the input information. Our research begins with several data normalization steps, including converting the sample to grayscale, eliminating noise, enhancing the spatial intensity, and outlining the sample contours. The results of these data normalization steps, we can attain Compressed Preprocessed Image (CPI), which is in the Fig.4(a), Fig.4(b), and Fig.4(c).

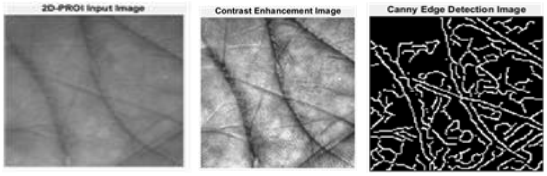

Fig.4. (a) 2DPROI Input Visual data (b) Contrast Enhancement Sample of 2DPROI Visual data (c) CPI of 2DPROI Visual data

Further, Compressed Contour Preprocessed Image of 2DPROI sample (CCPI) can be created using the Progressive Amalgamation of Conventional Compression (PACC) model on the CPI. The PACC model combines two conventional compression methods, DWT and PCA in a progressive manner. The Fig.5 shows the graphical representation of the PACC model. This intended PACC model reduces the CPI visual data, sized 128×128, to a CCPI sample of size 64×16. The details of the PACC procedure are outlined in section 3.3.1.

2.2.1 PACC Model is Implemented as follows:

The PACC model is a composite of DWT-PCA model, applied on CPI which as follows:

- At the first level of DWT, CPI is transformed into four sub and Visual data: LL_1, HL_1, LH_1, and HH_1.
- In the subsequent level of wavelet-based decomposition, LL_1 is again decomposed into four sub-bands: LL_2, HL_2, LH_2, and HH_2.

- In the next level of wavelet based decomposition, LL_2 is once again broken down into four sub-bands: LL_3, HL_3, LH_3, and HH_3.
- The dimensionality of LL_3 is reduced using the PCA model, final in the CCPI, as illustrated in Fig.5.

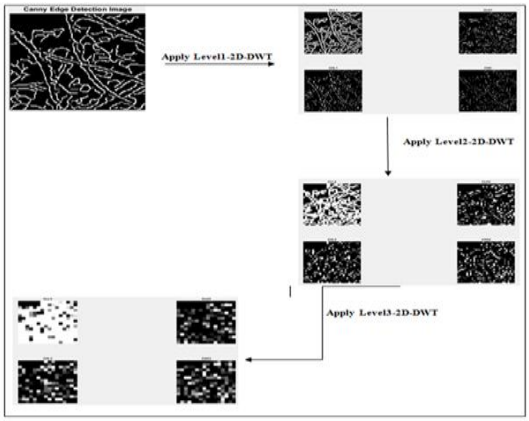

Fig.5. Formation of CCPI Using PACC Model

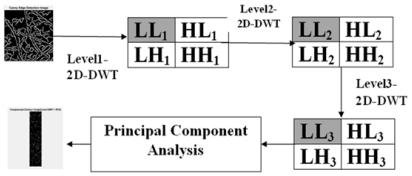

Fig.6. Pictorial Representation of PACC Model Implementation

2.3 ATTRIBUTE EXTRACTION LEVEL

HCCTA approach is used in this research to extract the proficient unique sample attribute values. It can be accomplished using the fusion of two texture features extraction approaches. The fusion of modal-based and statistical-based texture features extraction approaches is used. This fusion produces the blending of attribute elements while keeping individuality, which is called as hybrid attribute values extraction. The HCCTA method is applied in this study to obtain unique sample attribute values. This is achieved by combining two texture attribute extraction methods. The blend of modal-based and statistical-based extraction techniques creates hybrid attribute values while preserving individual characteristics. In the modal-based approach, the lacunarity value estimation method is employed, while the statistical-based extraction focuses on Haralick's features derived from CCPI Visual data.

2.3.1 Statistical-Based Texture Features Extraction Approach:

[21] Second-order statistical texture features of a sample can be obtained using the Compressed Contour Gray-Scale Level Co-occurrence Matrix (CCGLCM). The first step in this process is to calculate the GLCM values at various angles (0°, 45°, 90°, 135°, 180°, 225°, 270°, and 315°) to analyze the high frequency of pixels. Generate the eight $CGLCM_{CCPI}$ matrices with eight different orientations such as:

$$\begin{aligned} &CGLCM_{CCPI}(d=2,\theta=0^{\circ})\\ &CGLCM_{CCPI}(d=2,\theta=45^{\circ})\\ &CGLCM_{CCPI}(d=2,\theta=90^{\circ})\\ &CGLCM_{CCPI}(d=2,\theta=135^{\circ})\\ &CGLCM_{CCPI}(d=2,\theta=180^{\circ})\\ &CGLCM_{CCPI}(d=2,\theta=225^{\circ})\\ &CGLCM_{CCPI}(d=2,\theta=275^{\circ})\\ &CGLCM_{CCPI}(d=2,\theta=315^{\circ}) \end{aligned} \quad (1)$$

Statistical methods are essential for defining second-order texture based on gray-scale intensity at each pixel in the visual data. Features derived from GLCM describe the relationships between gray-scale pixels. Second-order methods typically offer better discrimination than other techniques [21]. Haralick et al. introduced 14 texture features from GLCM matrices in 1973. The second-order statistics features are extracted from the eight CGLCMs described in sections 3.3.2 and 3.3.3. Key features from Haralick's work, such as energy, contrast, homogeneity, entropy, and correlation, highlight the spatial relationships of gray levels between pixels in the normalized CGLCMs, revealing different aspects of texture information [21].

2.3.2 Feasible Haralicks' Features Extraction:

G is the number of gray levels used in the $CGLCM_{CCPI}$. $NCGLCM_{CCPI_m}$ is computed from eight $CGLCM_{CCPI}$ matrices using Eq.(2), where m represents as an index value of eight CGLCM. μ is the mean value of $NCGLCM_{CCPI_m}$ μ_x, μ_y, σ_x and σ_y are the means and standard deviations of $NCGLCM_{CCPI_m x}$ and $NCGLCM_{CCPI_m y}$ using Eq.(7), Eq.(8), Eq.(9), and Eq.(10). $NCGLCM_{CCPI_m x}(i)$ and $NCGLCM_{CCPI_m x}(j)$ is the i^{th} and j^{th} entry in the normalized eight $CGLCM_{CCPI}$ matrix using Eq.(5) and Eq.(6).

$$NCGLCM_{CCPI}^{(m)}(i,j)=\frac{CGLCM_{CCPI}^{(m)}(i,j)}{\sum_{i=0}^{G-1}\sum_{j=0}^{G-1}CGLCM_{CCPI}^{(m)}(i,j)} \quad (2)$$

$$S=\sum_{i=0}^{G-1}\sum_{j=0}^{G-1}CGLCM_{CCPI}^{(m)}(i,j) \quad (3)$$

$$NCGLCM_{CCPI}^{(m)}(i,j)=\frac{CGLCM_{CCPI}^{(m)}(i,j)}{S} \quad (4)$$

$$NCGLCM_{x}^{(m)}(i)=\sum_{j=0}^{G-1}NCGLCM_{CCPI}^{(m)}(i,j) \quad (5)$$

$$NCGLCM_{y}^{(m)}(j)=\sum_{i=0}^{G-1}NCGLCM_{CCPI}^{(m)}(i,j) \quad (6)$$

$$\mu_x=\sum_{i=0}^{G-1}i\,NCGLCM_{x}^{(m)}(i) \quad (7)$$

$$\mu_y=\sum_{j=0}^{G-1}j\,NCGLCM_{y}^{(m)}(j) \quad (8)$$

$$\sigma_x = \sqrt{\sum_{i=0}^{G-1}\sum_{j=0}^{G-1}(i-\mu_x)^2\, NCGLCM_{CCPI}^{(m)}(i,j)} \quad (9)$$

$$\sigma_y = \sqrt{\sum_{i=0}^{G-1}\sum_{j=0}^{G-1}(j-\mu_y)^2\, NCGLCM_{CCPI}^{(m)}(i,j)} \quad (10)$$

2.3.3 Fetching Feasible Haralick's Features:

- **Contrast:** The difference between the dark and light areas between a pixel and its neighborhood in $NCGLCM_{CC_{PI}}$ of an sample is calculated.

$$\text{Contrast} = \sum_{i=0}^{G-1}\sum_{j=0}^{G-1}(i-j)^2\, NCGLCM_{CCPI}^{(m)}(i,j) \quad (11)$$

- **Correlation:** It is defined as the connection of a pixel is to its neighborhood pixels.

$$\text{Correlation} = \frac{\sum_{i=0}^{G-1}\sum_{j=0}^{G-1}(i-\mu_x)(j-\mu_y)\, NCGLCM_{CCPI}^{(m)}(i,j)}{\sigma_x\sigma_y} \quad (12)$$

- **Energy:** It is an amount of squared components in $NCGLCM_{\text{CC}_{\text{PI}}}$.

$$\text{Energy} = \sum_{i=0}^{G-1}\sum_{j=0}^{G-1}\left[NCGLCM_{CCPI}^{(m)}(i,j)\right]^2 \quad (13)$$

- **Homogeneity:** It gives a thought regarding the closeness of components in $NCGLCM_{\text{CC}_{\text{PI}}}$ to its corner-to-corner component.

$$\text{Homogeneity} = \sum_{i=0}^{G-1}\sum_{j=0}^{G-1}\frac{NCGLCM_{CCPI}^{(m)}(i,j)}{1+|\,i-j|} \quad (14)$$

- **Entropy:** Sample entropy is an amount which is utilized to depict how much data which should be coded by a compression model.

$$\text{Entropy} = -\sum_{i=0}^{G-1}\sum_{j=0}^{G-1}NCGLCM_{CCPI}^{(m)}(i,j)\log\left(NCGLCM_{CCPI}^{(m)}(i,j)\right) \quad (15)$$

In this way, the five Haralick's element values are made out and put away as the training and testing templates utilizing CGLCM approach.

2.3.4 Modal-Based Texture Features Extraction Approach:

Adaptive analysis in the spatial dependence of the pixel intensities in the CCPI sample are used to construct training and testing templates. These spatial intensity changes are regarded as texture features and contain both redundant and non-redundant sample information value [53]. Model-based methods also provide a consistent way of representing the attributes of fractals and retain uniformity over textures and dimensions to extract texture-specific information [53]. Lacunarity is a supplementary descriptor to distinguish between spatial patterns with same Fractal Dimension (FD) values. [54] integrated the competition process with multi-order texture features and developed CCNet to achieve a remarkable performance on four public datasets and proved that CCNet is a promising approach for palmprint recognition that can achieve state-of-the-art performance. The idea of lacunarity was intended by Mandelbrot to compensate for the differences in texture appearance that may potentially exist even if a given local FD is similar, by representing a set of variances or mean values— that is, multiple lacunarity texture values. As introduced in [55], the gliding-box model has proven to be effective in modeling the complexity and diversity of coarse texture patterns. Lacunarity is calculated using the mass distribution function with the gliding-box model, as explained in [55].

2.3.5 Framework for Lacunarity ($\mathscr{L}$) estimation in EPI analysis

- At primitive CCPI image size is $\acute{S}\times\acute{S}$. In the Gliding-box algorithm, the $\mathscr{L}$ value is determined for every gliding box. Each gliding box is formed by shifting one edge to the front and adjusting the lower edge, resulting in non-overlapping boxes of dimensions $\eta\times\eta$, where η varies from 1 to $\acute{S}/\Phi$. These boxes are derived from the upper left corner of the CCPI visual data. The scale interval, represented as Φ, spans from 1 to $\log2(\acute{S})/2$.
- For every gliding box, the pixel density weight is calculated using the mass ratio ($mr(\eta,\Phi)$). This involves dividing the total intensity values (pw_η) of the occupied gray-scale pixels within each overlapping box by the total number of boxes (Nb_η). This computation can be executed using Eq.(16).

$$mr(\eta,\Phi) = \sum_{i=1}^{\frac{\log_2(\bar{S})}{2}}\frac{pw_\eta}{N_{b,\eta}}\,\middle|\,\Phi=1,2,\ldots,\left\lfloor\frac{\log_2(\bar{S})}{2}\right\rfloor\,\middle|\,\eta=1,2,\ldots,\frac{\bar{S}}{\Phi} \quad (16)$$

Lacunarity ($\mathscr{L}_\Phi$) at different scales Φ can be calculated using the Eq.(17).

$$\mathrm{L}_\Phi = \frac{\sum_{i=1}^{\frac{\log_2(\bar{S})}{2}} mr(\eta,\Phi)^2\times CCPI_{(\eta,\Phi)}}{\sum_{i=1}^{\frac{\log_2(\bar{S})}{2}}\left[mr(\eta,\Phi)\times CCPI_{(\eta,\Phi)}\right]^2}\,\middle|\,\Phi=1,2,\ldots,\frac{\log_2(\bar{S})}{2}\,\middle|\,\eta=1,2,\ldots,\frac{\bar{S}}{\Phi} \quad (17)$$

The Lacunarity $\mathscr{L}_\Phi$ attribute vector is computed for a test visual data, final in a dimension of 1×3. This process is similarly applied to all training and testing visual data to obtain their respective $\mathscr{L}_\Phi$ values. Subsequently, all extracted attribute values, derived from both statistical and modal-based texture attribute methods, are consolidated into a single attribute vector. This consolidation leads to the formation of training and testing templates, which are essential for the authentication and identification processes within the HCCTA-PRS model.

2.4 CLASSIFICATION OR MATCHING LEVEL

This research paper details the creation of the SDLC_{Net} classifier, which is engineered to effectively recognize and classify visual data through a supervised learning framework. The design of the classifier is based on a Deep Neural Network (DNN), including input, processing or hidden, and terminal or output layers, each configured with a particular number of perceptrons. To enhance the performance, the architecture is fine-tuned by varying the number of processing layers and perceptrons, aiming to reduce error rates during the training phase. Essential elements of the training process, such as the learning rate and epoch values, play a significant role in guiding

gradient descent and determining the necessary iterations to achieve minimal mean square error. The weight matrices within the DNN are pivotal for the learning process, with updates occurring through forward and backward passes to calculate prediction errors and gradients. Following a supervised learning methodology, hyper-parameters, especially the learning rate, are crucial for the convergence of model weights. $SDLC_{Net}$ incorporates the Non-linear Rectified Linear Unit activation function in its processing layers and employs the Sigmoid function for the output layer, thereby improving both performance and stability. Once trained, $SDLC_{Net}$ operates as a classification model, capable of predicting outputs for new inputs and facilitating performance assessment based on these predictions.

3. EXPERIMENTAL ANALYSIS

This study uses 400 2DPROI visual data from 20 workers in the POLYU dataset. Of these, 80% are allocated for training and 20% for testing in the palmprint identification process. During the testing phase, 100 test visual data are created initially and increased by 100 for each subsequent test. The HCCTA attribute extraction method is used to generate the training and testing templates. In this HCCTA method, the input sample of size (128 × 128) is reduced to a CCPI sample of size (16 × 16) using the PACC model, which emphasizes essential, features for quicker processing times. The Fig.8 illustrates this process. The PACC model employs Level 3-DWT, where both detailed (D) and approximated (A) visual data are produced at each level. The detailed sample from each level is carried on to the next DWT stage to create a finely compressed detailed visual data, as shown in Figure 7.

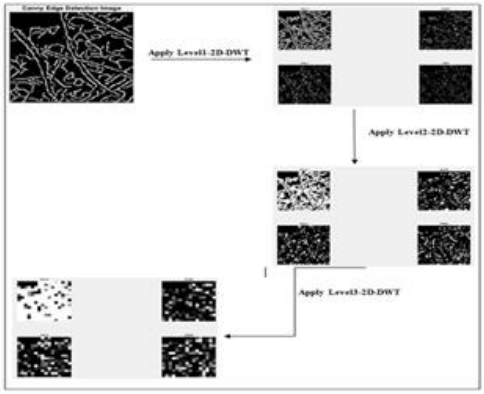

Fig.7. Resultant of Level3 DWT Model of CCPI Visual data

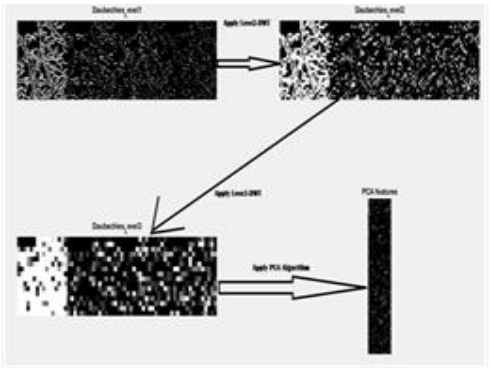

Fig.8. Formation of CCPI Using PACC Model

The CCPI sample is used to extract second-order texture features for creating training and testing templates. Initially, eight Gray Level Co-occurrence Matrices (GLCMs) are generated from the CCPI sample at various orientations. From the normalized GLCM, five Haralick features are extracted: Contrast, Homogeneity, Energy, Entropy, and Correlation. The calculated values of these features are 0.50741, 0.02637, 0.532286, 0.851709, and 3.892496. The lacunarity values are estimated using the Gliding-Box model, yielding a lacunarity value of 5.1713 for the test visual data. This process results in a attribute vector containing six attributes that form the training and testing templates.

During the training phase, features from 400 2DPROI visual data are extracted. The $SDLC_{Net}$ classifier comprises one input layer, one terminal layer, and five processing layers. The input layer has six nodes that hold the five Haralick attribute values and one lacunarity value. The output layer consists of $\lfloor \log_2(n) \rfloor + 2$ nodes, where n is the maximum number of training datasets used. Seven processing layers are included in the $SDLC_{Net}$ classifier. After establishing the $SDLC_{Net}$, a supervised model known as BPANN are applied to create the HCCTA-$SDLC_{Net}$ PRS model. The learning process is deemed complete when the lowest Mean Square Error (MSE) values are achieved, as shown in the training performance graph Fig.10. The learning process of the $SDLC_{Net}$ classifier is completed at epoch 7000, reaching the minimum MSE. The specifications of the trained $SDLC_{Net}$ classifier are detailed in Table.2.

Table.2. Peculiar Arguments of $SDLC_{Net}$ Classifier during the Learning Process of HCCTA-$SDLC_{Net}$ PRS Model

Parameter	Value
Number of Authenticating Visual Data	400
Number of Training Factors (Input Nodes)	6
Number of Output Nodes	10
Number of Passes	7000
Number of Processing Layers	7
Number of Processing Nodes	45
Learning Rate	0.00001

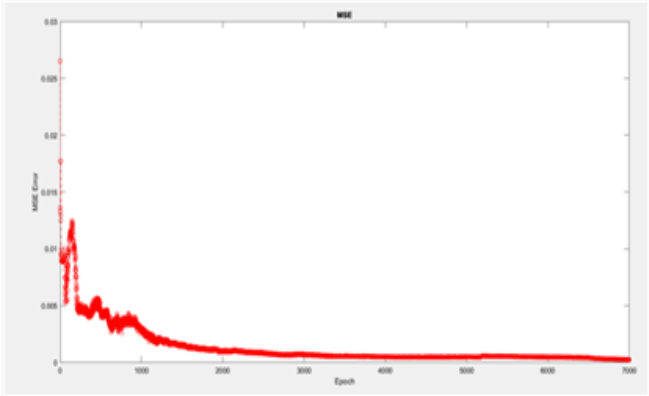

Fig.10. $SDLC_{Net}$ Classifier Performance Graph

The efficiency of the HCCTA-$SDLC_{Net}$ PRS Model is analyzed using aspects of the confusion matrix. Those aspects are Accuracy, True Positive Rate (TPR), and False Positive Rate

(FPR). The values of these aspects are calculated by applying the diagnostic variables on metric formula: True Positive (TP), True Negative (TN), Type1 error, and Type2 error. The values for these diagnostic variables may be identified by analyzing the correctly matched and mismatched records within the authenticated dataset compared to the template datasets.

Table.3 and Fig.11 show the increasing values of TPR (0.9897, 0.9944, 0.9961, 0.9971) and CPR (0.98, 0.99, 0.99, 0.9950) across all testing datasets. Table.3 indicates that the HCCTA-SDLC$_{Net}$ PRS Model accurately classifies large datasets. Table.4 and Fig.12 present the performance of the HCCTA-SDLC$_{Net}$ PRS Model compared to existing biometric systems in terms of recognition rates. This demonstrates that the intended system is among the most effective for accurately identifying authorized individuals.

4. DISCUSSION

The research aims to positively impact society by developing effective recognition methods to an efficient PRS model. Tables.3 and 4 present the performance of the HCCTA-SDLC$_{Net}$ PRS Model and compare its authentication accuracy with other existing recognition techniques. This comparison highlights the improvements in performance. The Fig.12 demonstrates that the HCCTA-SDLC$_{Net}$ PRS Model achieves a 99.50% authentication accuracy rate, surpassing other methods in current biometric technologies. Therefore, the HCCTA-SDLC$_{Net}$ PRS Model can be considered among the best systems for securing access to authenticated data and information.

Table.3. The model's estimated outputs along with the evaluation metrics derived from the confusion matrix

Total No. of samples taken	TP	TN	Type 1 error	Type 2 error	TPR	FPR	Accuracy (CPR)
100	96	2	1	1	98.97%	33.33%	98.00%
200	178	20	1	1	99.44%	4.76%	99.00%
300	258	39	2	1	99.61%	4.88%	99.00%
400	343	55	1	1	99.71%	1.79%	99.50%

Table 2. Comparative Analysis of Existing Recognition Approaches with Intended Approaches

Recognition Approaches	Authentication Accuracy Rate	Publication Year
DWT + GLCM Attribute Extraction Approach and KNN Classifier [56]	95.7%	2010
DMWT + LBP +PCA Attribute Extraction Approach and Euclidean Distance Classifier [57]	98.4%	2011
Haar Wavelet Transform + GLCM Attribute Extraction Approach, Random Forest Classifier [58]	97.39%	2019
GLCM Attribute Extraction Approach +DNN Classifier [59]	98%	2020
GLCM and DWT Attribute Extraction Approach and CNN Classifier [60]	91%	2020
DWT + GLCM Attribute Extraction Approach, and SVM + RBF Classifier [61]	93.62%	2021
Fractal Dimension, Lacunarity, LBP Histogram, Mean Intensity and Contrast [62]	90.5%	2021
Generalized Dimensions + Lacunarity + Singularity Spectrum + SVM Classifier [63]	98.5%	2021
3CGLCM-Cnn$_{net}$ System DWT + PCA + GLCM Haralick's Features Extraction Approach (3CGLCM) and CNN Classifier [21]	99%	2023
SCLA-WALBP + DlNSA$_{Net}$ Classifier [64]	99%	2023
Intended Approaches HCCTA + SDLC$_{Net}$ Classifier	**99.50%**	-

5. CONCLUSION

The intended HCCTA-SDLC$_{Net}$ PRS model aims to extract valuable features through a combined approach of model-based and statistic-based techniques. It uses SDLC$_{Net}$ classifier for accurate person recognition from low-dimensional CCPI Visual data, utilizing the PACC model. This research is conducted on the 400 POLYU 2D-PROI dataset, allocating 80% for training and 20% for testing. The recognition rate of the intended system is 99.50%, which surpasses existing systems, indicating the effectiveness of HCCTA-SDLC$_{Net}$ as a reliable PRS. Future research will focus on enhancing the attribute selection and extraction processes to improve recognition accuracy to 100%, making it a significant advancement in biometric technology.

REFERENCES

[1] A. Kamboj, R. Rani and A.A. Nigam, "Comprehensive Survey and Deep Learning-based Approach for Human Recognition using Ear Biometric", *Visual Computer*, Vol. 38, No. 7, pp. 2383-2416, 2022.

[2] Kah Ong Michael Goh, Tee Connie and Andrew Teoh, "Touch-Less Palm Print Biometric System", *Proceedings of International Conference on Computer Vision Theory and Applications*, Vol. 2, pp. 423-430, 2008.

[3] L. Fei, B. Zhang, W. Jia, J. Wen and D. Zhang, "Attribute Extraction for 3-D Palmprint Recognition: A Survey", *IEEE Transactions on Instrumentation and Measurement*, Vol. 69, No. 3, pp. 645-656, 2020.

[4] J. Gururaj and B. Prashant, "Biometric Recognition of Humans using Scanned Visual Data of the Retinal Part of the Eyes", *International Journal of Future Generation Communication and Networking*, Vol. 13, No. 1, pp. 1055-1071, 2020.

[5] L. Wayman, "Fundamentals of Biometric Authentication Technologies", *International Journal of Image and Graphics*, Vol. 1, No. 1, pp. 93-113, 2001.

[6] J.A. Unar, W.C. Seng and A.A. Abbasi, "A Review of Biometric Technology along with Trends and Prospects", *Pattern Recognition*, Vol. 47, No. 8, pp. 2673-2688, 2014.

[7] A. Kong, D. Zhang and M. Kamel, "A Survey of Palmprint Recognition", *Pattern Recognition*, Vol. 42, pp. 1408-1418, 2009.

[8] Y.P. Wu, J.W. Tian and D. Xu, "Palmprint Recognition based on RBK-Means and Hierarchical SVM", *Proceedings of International Conference on Machine Learning and Cybernetics*, Vol. 6, pp. 1-11, 2007.

[9] W. El-Tarhouni, L. Boubchir, M. Elbendak and A. Bouridane, "Multispectral Palmprint Recognition using Pascal Coefficients-based LBP and PHOG Descriptors with Random Sampling", *Neural Computing and Applications*, Vol. 31, No. 2, pp. 593-603, 2019.

[10] Adams Kong, David Zhang and Guangming Lu, "A Study of Identical Twins Palmprint for Personal Verification", *Pattern Recognition*, Vol. 39, No. 11, pp. 2149-2156, 2006.

[11] M.M.H. Ali, P. Yannawar and A.T. Gaikwad, "Study of Edge Detection Methods based on Palmprint Lines", *Proceedings of International Conference on Electrical, Electronics and Optimization Techniques*, Vol. 8, No. 2, pp. 1-7, 2016.

[12] K.N. Bharath, G. Padmajadevi and Kiran, "Hybrid Compression using DWT-DCT and Huffman Encoding Techniques for Biomedical Sample and Video Applications", *International Journal of Computer Science and Mobile Computing*, Vol. 2, No. 5, pp. 255-261, 2013.

[13] I. Daubechies, "*Ten Lectures on Wavelets*", 1992.

[14] R.S. Chowdhury, J. Jana, S. Tripathi and J. Bhaumik, "Improved DWT and IDWT Architectures for Image Compression", *Microprocessors and Microsystems*, Vol. 104, pp. 1-9, 2023.

[15] R. Ranjan and P. Kumar, "An Improved Image Compression Algorithm using 2D DWT and PCA with Canonical Huffman Encoding", *Entropy*, Vol. 25, No. 10, pp. 1-24, 2023.

[16] G. Kaur and K. Kaur, "Image Compression using DWT and Principal Component Analysis", *IOSR Journal of Electrical and Electronics Engineering*, Vol. 10, No. 3, pp. 53-56, 2015.

[17] M. Kakore, P.K. Biswas and B.N. Chatterjee, "Texture Sample Retrieval using Rotated Wavelet Filters", *Pattern Recognition Letters*, Vol. 28, pp. 1240-1249, 2007.

[18] A.A. Mohammed and J.A. Hussein, "Efficient Hybrid Transform Scheme for Medical Sample Compression", *International Journal of Computer Applications*, Vol. 27, pp. 16-20, 2011.

[19] Figlu Mohanty, Suvendu Rup, Bodhisattva Dash, Banshidhar Majhi and M.N.S. Swamy, "Digital Mammogram Classification using 2D-BDWT and GLCM Features with FOA-based Attribute Selection Approach", *Neural Computing and Applications*, Vol. 32, pp. 7029-7043, 2019.

[20] B. Abirami and K. Krishnaveni, "Compressed Contour Cumulative GLCM Texture Analysis Model based CNN for Palmprint Recognition System", *Journal of Data Acquisition and Processing*, Vol. 38, No. 2, pp. 923-941, 2023.

[21] Ajay Kumar, C.M. David Wong, C. Helen Shen and K. Anil Jain, "Personal Verification using Palmprint and Geometry Biometric", *Proceedings of International Conference on Audio and Video-Based Biometric Person Authentication*, Vol. 2688, pp. 668-678, 2003.

[22] A. Kumar and D. Zhang, "Integrating Shape and Texture for Hand Verification", *Proceedings of International Conference on Sample and Graphics*, Vol. 6, pp. 222-225, 2004.

[23] A. Bruno, P. Carminetti, V. Gentile, M. La Cascia and E. Mancino, "Palmprint Principal Lines Extraction", *Proceedings of International Workshop on Biometric Measurements and Systems for Security and Medical Applications*, Vol. 13, pp. 50-56, 2014.

[24] Anne Humeau-Heurtier, "Texture Attribute Extraction Methods: A Survey", *IEEE Access*, Vol. 7, pp. 8975-9000, 2019.

[25] T. Ojala, M. Pietikainen and D. Harwood, "A Comparative Study of Texture Measures with Classification based on Featured Distributions", *Pattern Recognition*, Vol. 29, No. 1, pp. 51-59, 1996.

[26] LalehArmi and Shervan Fekri-Ershad, "Texture Sample Analysis and Texture Sample Analysis and Texture Classification Methods-A Review", *International Online Journal of Sample Processing and Pattern Recognition* Vol. 2, No. 1, pp. 1-29, 2019.

[27] Mrinal Kanti Bhowmik, Anindita Roy, Usha Rani Gogoi and Niharika Nath, "Estimation of Architectural Distortion in Mammograms using Fractal Features", *Proceedings of International Conference on Medical Imaging*, Vol. 13, No. 6, pp. 21-37, 2017.

[28] R. Mokini and K. Monji, "Palmprint Recognition through the Fractal Dimension Estimation for Texture Analysis", *International Journal of Biometrics*, Vol. 8, No. 4, pp. 254-274, 2016.

[29] M. Raouia, D. Hassen and K. Monji, "Deep-Analysis of Palmprint Representation based on Correlation Concept for Human Biometrics Identification", *International Journal of Digital Crime and Forensics*, Vol. 10, pp. 1-19, 2020.

[30] X. Shi, H.D. Cheng, L. Hu, W. Ju and J. Tian, "Detection and Classification of Masses in Breast Ultrasound Visual Data", *Digital Signal Process*, Vol. 20, No. 3, pp. 824-836, 2010.

[31] Gun-Baek So, Hye-Rim So and Gang-Gyoo Jin, "Enhancement of the Box-Counting Model for Fractal Dimension Estimation", *Pattern Recognition Letters*, Vol. 98, pp. 53-58, 2017.

[32] M.N. Barros Filho and F.J.A. Sobreira, "Accuracy of Lacunarity Models in Texture Classification of High Spatial Resolution Visual Data from Urban Areas", *The International Archives of the Photogrammetry, Remote Sensing and Spatial Information Sciences*, Vol. 2, No. 3, pp. 1-8, 2008.

[33] S.W. Myint and N. Lam, "A Study of Lacunarity based Texture Analysis Approach to Improve the Urban Sample Classification", *Computers Environment and Urban Systems*, Vol. 29, No. 5, pp. 501-523, 2005.

[34] Xiong He, Zijiang Yang and Kun Zhang, "Research on Urban Expansion Methods based on Lacunarity Index", *Proceedings of International Conference Geo Informatics and Data Analysis*, Vol. 7, No. 8, pp. 93-98, 2019.

[35] R. Charles Tolle, R. Timothy McJunkin and J. David Gorsich, "An Efficient Implementation of the Gliding Box

Lacunarity Algorithm", *Physica D: Nonlinear Phenomena*, Vol. 237, No. 3, pp. 306-315, 2008.

[36] Mohammad Keyvanpour, Shokofeh Vahidiansadegh and Zahra Mirzakhani, "An Analytical Review of Texture Feature Extraction Approaches", *International Journal of Computer Applications in Technology*, Vol. 65, No. 2, pp. 118-133, 2021.

[37] R.M. Haralick, K. Shanmugam and I. Dinstein, "Textural Features for Image Classification", *IEEE Transactions on Systems, Man and Cybernetics*, Vol. 3, No. 6, pp. 610-621, 1973.

[38] Dipankar Hazra, "Texture Recognition with Combined GLCM, Wavelet and Rotated Wavelet Features", *International Journal of Computer and Electrical Engineering*, Vol. 3, No. 1, pp. 146-150, 2011.

[39] Taner Cevik, Ali Mustafa Alshaykha and Nazife Cevik, "A Comprehensive Performance Analysis of GLCM-DWT-based Classification on Fingerprint Identification", *International Journal of Computer Applications*, Vol. 180, No. 32, pp. 42-47, 2018.

[40] Q. Tian, N. Sebe, M.S. Lew, E. Loupias and T.S. Huang, "Image Retrieval using Wavelet-based Salient Points", *Journal of Electronic Imaging, Special Issue on Storage and Retrieval of Digital Media*, Vol. 10, No. 4, pp. 835-849, 2001.

[41] Tianhorng Chang and C.C. Jay Kuo, "Texture Analysis and Classification with Tree-Structured Wavelet Transform", *IEEE Transactions on Image Processing*, Vol. 2, No. 4, pp. 429-441, 1993.

[42] L. Li, J. Yang, L.Y. Por, M.S. Khan, R. Hamdaoui, L. Hussain, Z. Iqbal, I.M. Rotaru, D. Dobrota, M. Aldrdery and A. Omar, "Enhancing Lung Cancer Detection through Hybrid Features and Machine Learning Hyperparameters Optimization Techniques", *Heliyon*, Vol. 10, No. 4, pp. 1-9, 2024.

[43] Annarita Fanizzi, Teresa Maria Basile, Liliana Losurdo, Roberto Bellotti, Ubaldo Bottigli, Francesco Campobasso, Vittorio Didonna, Alfonso Fausto, Raffaella Massafra, Alberto Tagliafico, Pasquale Tamborra, Sabina Tangaro, Vito Lorusso and Daniele La Forgia, "Ensemble Discrete Wavelet Transform and Gray-Level Co-Occurrence Matrix for Microcalcification Cluster Classification in Digital Mammography", *Applied Sciences*, Vol. 9, No. 24, pp. 1-14, 2019.

[44] Shankar Bhausaheb Nikam and Suneeta Agarwal, "Wavelet Energy Signature and GLCM Features-based Fingerprint Anti-Spoofing", *Proceedings of International Conference on Wavelet Analysis and Pattern Recognition*, Vol. 3, No. 1, pp. 1-9, 2008.

[45] R.F. Chang, C.J. Chen and M.F. Ho, "Breast Ultrasound Image Classification using Fractal Analysis", *Proceedings of International Symposium on Bioinformatics and Bioengineering*, Vol. 8, No. 3, pp. 1-6, 2004.

[46] M.M. Ata, K.M. Elgamily and M.A. Mohemed, "Toward Palmprint Recognition Methodology based Machine Learning Techniques", *European Journal of Electrical Engineering and Computer Science*, Vol. 4, No. 4, pp. 1-10, 2020.

[47] B. Ordek, Y. Borgianni and E. Coatanea, "Machine Learning-Supported Manufacturing: A Review and Directions for Future Research", *Production and Manufacturing Research*, Vol. 12, No. 1, pp. 1-9, 2024.

[48] Z. Dandan, P. Xin, L. Xiaoling and G. Xiaojing, "Palmprint Recognition based on Deep Learning", *Proceedings of International Conference on Wireless, Mobile and Multi-Media*, Vol. 3, No. 1, pp. 1-6, 2015.

[49] Y. LeCun, Y. Bengio and G. Hinton, "Deep Learning", *Nature*, Vol. 521, pp. 436-444, 2015.

[50] B. Abirami and K. Krishnaveni, "A Deep Convolution Multifractal Analysis using Principle Line Extraction Approach for Palmprint Recognition System", *Proceedings of International Conference on Computational Electronics for Wireless Communications*, Vol. 959, pp. 293-308, 2024.

[51] Z. Yang, H. Huangfu, L. Leng, B. Zhang, A.B.J. Teoh and Y. Zhang, "Comprehensive Competition Mechanism in Palmprint Recognition", *IEEE Transactions on Information Forensics and Security*, Vol. 18, pp. 5160-5170, 2023.

[52] P. Dong, "Test of a New Lacunarity Estimation Method for Sample Texture Analysis", *International Journal of Remote Sensing*, Vol. 21, No. 17, pp. 3369-3373, 2000.

[53] B. Gopinath and B.R. Gupta, "Majority Voting based Classification of Thyroid Carcinoma", *Procedia Computer Science*, Vol. 2, pp. 265-271, 2010.

[54] Li Yunfeng and Zhang Yali, "Palmprint Recognition based on Weighted Fusion of DMWT and LBP", *Proceedings of International Congress on Image and Signal Processing*, Vol. 3, pp. 1-7, 2011.

[55] Sujata, Rajesh Parihar and Vikas Sharma, "Detection and Classification of Tumor Type in Brain MRI Visual Data using SVM and Deep Learning Techniques", *Proceedings of International Conference on Machine Learning*, Vol. 16, No. 10, pp. 1-9, 2020.

[56] Alpana Jijja and Dinesh Rai, "Segmentation of Brain Tumor using GLCM and Discrete Wavelet Transform", *International Journal of Innovative Technology and Exploring Engineering*, Vol. 9, No. 6, pp. 1-7, 2020.

[57] Oliver Faust, Joel En Wei Koh, Vicnesh Jahmunah, Sukant Sabut, J. Edward Ciaccio, Arshad Majid, Ali Ali, Y.H. Gregory Lip and U. Rajendra Acharya, "Fusion of Higher Order Spectra and Texture Extraction Methods for Automated Stroke Severity Classification with MRI Visual Data", *International Journal of Environmental. Research and Public Health*, Vol. 18, No. 15, pp. 1-19, 2021.

[58] A. Concea, T. Nitescu, L. Ichim and D. Popescu, "Texture Analysis for Visual data with Forested Areas", *Proceedings of International Conference on Control Systems and Computer Science*, Vol. 8, pp. 197-202, 2021.

[59] M.M. Abdelsalam and M.A. Zahran, "A Novel Approach of Diabetic Retinopathy Early Detection based on Multifractal Geometry Analysis for OCTA Macular Visual Data using Support Vector Machine", *IEEE Access*, Vol. 9, pp. 22844-22858, 2021.

[60] B. Abirami and A. Krishnaveni, "A Deep Supervised Lacunarity Analysis Model based on Weight Adaptive Local Binary Pattern Texture for Palmprint Recognition System", *Journal of Pharmaceutical Negative Results*, Vol. 14, No. 3, pp. 1984-1995, 2023.